AIAA 79-1811R

Performance Evaluation of an Air Vehicle Utilizing Nonaxisymmetric Nozzles

J. A. Laughrey*
Wright Aeronautical Laboratories, Wright-Patterson Air Force Base, Ohio
and
D. J. Drape† and P. E. Hiley‡
McDonnell Aircraft Company, St. Louis, Mo.

An extensive nonaxisymmetric nozzle design and performance data base were utilized to evaluate the performance of a vehicle designed for an air-to-air mission. Performance was evaluated through comparative sizing analysis for selected nonaxisymmetric nozzle installations vs a baseline axisymmetric nozzle installation. The nonaxisymmetric nozzle/vehicle with a single, external expansion ramp was found to be lighter in takeoff gross weight (TOGW) than the axisymmetric baseline. The lighter TOGW resulted primarily from the use of thrust vectoring at the transonic maneuver condition used for engine sizing. Both jet lift and thrust-induced lift or supercirculation were the main contributors to improved performance at this flight condition.

Nomenclature

$\bar{c}$	= wing mean aerodynamic chord
C_D	= drag coefficient, D/qS_w
$C_{D_{noz}}$	= nozzle drag coefficient
$C_{D_{MP}}$	= minimum profile drag
$\Delta D_{D_{noz}}$	= throttle dependent drag increment
$\Delta C_{D_{ref}}$	= drag increment between axi and 2-D reference nozzles of 0 deg angle of attack
C_{F_g}	= nozzle resultant gross thrust coefficient, F_g/F_{ideal}
$\Delta_{CF_{g_{cooling}}}$	= change in C_{F_g} due to cooling of nozzles and afterburner
$C_{F_{g_{ins}}}$	= installed C_{F_g} (model data corrected for full-scale cooling and leakage effects)
$\Delta C_{F_{g_{leakage}}}$	= change in C_{F_g} due to leakage in nozzle
$C_{F_{g_{model}}}$	= measured C_{F_g}
C_L	= lift coefficient, L/qS_w
C_m	= pitching moment coefficient, $PM/qS_w\bar{c}$
C_T	= thrust coefficient, F_g/qS_w
F_g	= nozzle resultant gross thrust
F_{ideal}	= nozzle ideal thrust for complete isentropic expansion of actual jet flow to ambient static pressure
g	= load factor
M	= freestream Mach number
NPR	= nozzle pressure ratio
psf	= pounds per square foot
q	= freestream dynamic pressure
S_w	= wing reference area
α	= angle of attack
β	= nozzle terminal boattail angle
δ_c	= canard deflection angle
δ_V	= measured gross thrust vector angle relative to horizontal plane

Subscripts

aero	= aerodynamic forces or moments (direct jet contributions removed)
ref	= reference conditions
tot	= total forces or moments (aerodynamic plus direct jet contributions)
trim	= trimmed condition
Γ	= thrust vector-induced aerodynamic force or moment increments referenced to unvectored, jet-on conditions

Presented as Paper 79-1811 at the AIAA Systems and Technology Meeting, New York, N.Y., Aug. 20-22, 1979; submitted Sept. 13, 1979; revision received May 15, 1980. This paper is declared a work of the U.S. Government and therefore is in the public domain.

*Aerospace Engineer. Member AIAA.
†Lead Engineer, Aerodynamics.
‡Section Chief, Propulsion.

Introduction

CRITICAL performance improvements desired in future fighter aircraft include increased maneuverability and agility at high angles of attack, reduction of subsonic and supersonic cruise drag, and a reduction in takeoff and landing distances. Recent investigations, involving the integration of the propulsion system with the airframe, have shown it is possible to improve fighter performance by incorporating nonaxisymmetric nozzles with thrust vectoring and/or reversing capability. Incorporation of vectorable nonaxisymmetric nozzles near the trailing edge of the wing can significantly enhance the overall lift, thereby improving maneuvering performance. Thrust reversing can greatly improve and control in-flight deceleration and can significantly shorten landing ground roll. It is also possible to reduce overall aircraft drag with the proper integration of nonaxisymmetric nozzles into the airframe.

During a recently completed program,[1] static[2,3] and wind tunnel tests[4] were conducted to determine the internal and installed performance characteristics of a baseline axisymmetric nozzle and various nonaxisymmetric nozzles shown in Fig. 1. The data base generated was utilized in a vehicle sizing evaluation of air-to-air fighter configurations having axisymmetric and nonaxisymmetric nozzles. The nozzle designs and experimental results are briefly described, followed by a summary of the performance evaluation approach and sizing results.

Nozzle Designs and Experimental Results

Feasible full-scale mechanical designs were generated by General Electric (GE) and Pratt and Whitney Aircraft Group (P&WA), Florida, along with five different nonaxisymmetric nozzle types and an axisymmetric baseline nozzle. Nozzle weight, leakage, and cooling estimates were also prepared.

Weight estimates for the full-scale nonaxisymmetric exhaust systems, some with vectoring capability and some with both reversing and vectoring, ranged from about 60 to 900 lb heavier than a nominal axisymmetric nozzle without

reversing or vectoring capability (weights at 160 lb/s design airflow for an advanced turbofan engine). The C-D and external expansion single ramp nozzles were the lightest concepts, with the plug weights considerably higher. Weight increases are caused primarily by the addition of vectoring/reversing capability, plus the inherently poor structural efficiency of two-dimensional compared to round shapes. However, the flat sidewall and flap systems of the 2-D designs make it possible to use more efficient nozzle cooling and sealing schemes, resulting in performance improvements compared to an axisymmetric nozzle.

All nozzle models were also tested in the propulsion wind tunnel (16 T) at AEDC on a NASA-supplied "test pod" jet effects model with a simple aerodynamic shape. The nozzle exits were aligned at the wing trailing edge to maximize thrust vectoring effects. Tests were conducted at three power setting simulations, thrust vector angles up to 30 deg (positive down from horizontal), and at dry power reverse thrust. Nozzle pressure ratios were varied consistent with the test Mach number.

The highest static internal performance was demonstrated for the nonaxisymmetric convergent-divergent (C-D) nozzle types, exhibiting gross thrust coefficient (C_{F_g}) values that were within 1% of the baseline axisymmetric nozzle. All nonaxisymmetric designs gave minimal performance losses due to vectoring at maneuver conditions, and reverse thrust levels up to 50% of maximum dry power forward thrust were measured on the C-D nozzle types. The wind tunnel test results indicated that the nonaxisymmetric nozzles with external expansion surfaces exhibited the highest thrust minus drag at unvectored cruise and maneuver conditions. Their performance was equal to or better than that for the axisymmetric baseline nozzle. Vectoring was found to improve the untrimmed lift to drag ratio for all nonaxisymmetric nozzles at all positive thrust vector angles. The lift, drag, and pitching moment increments induced on the wing/body by vectoring were shown to correlate well with modified trailing edge flap theory.

Vehicle Performance Evaluations

Following the static and wind tunnel tests, use of the nozzle design and performance data base was demonstrated in vehicle sizing evaluations. Three of the tested nonaxisymmetric nozzles were chosen for sizing analysis on advanced fighters designed for an air-to-surface (A/S) and an air-to-air (A/A) mission. The baseline for comparison on both fighters was the advanced axisymmetric nozzle installation. In the following, the A/A mission and full-scale nozzle/vehicle designs are described as well as the prediction of the aerodynamic and gross thrust performance and the vehicle sizing results.

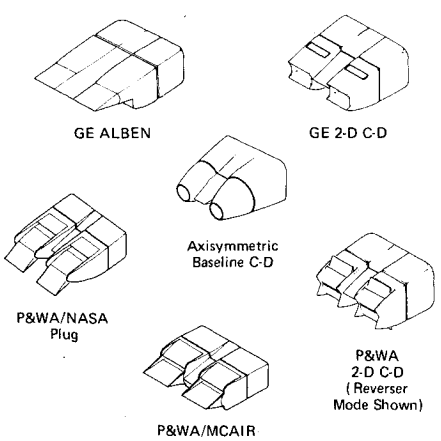

Fig. 1 Exhaust nozzle types investigated.

Mission Description

The A/A mission, depicted in Fig. 2, is characterized by high altitude subsonic cruise and demanding transonic turn requirements. The most critical flight conditions for the A/A mission, as defined by the fuel consumption requirements over the various mission segments, are shown in Table 1. Other important flight conditions, corresponding to point design requirements for transonic maneuvering and maximum speed (V_{max}), are the 6 g sustained turn at Mach 0.9/30,000 ft and the V_{max} condition at Mach 1.8/36,089 ft.

Full-Scale Vehicle and Nozzle Descriptions

The important features of the vehicle designed to satisfy the requirements of the A/A mission are shown in Fig. 3. This configuration is a close-coupled canard/wing concept characterized by low wing loading and wide-spaced, podded engine/nozzle installation. This installation permits attractive integration of high aspect ratio nonaxisymmetric nozzles as well as the low aspect ratio designs of the subject study.

The A/A vehicle incorporates an advanced, mixed flow turbofan with moderate bypass ratio (~0.90) and afterburning capability. The engine cycle remained unchanged for all nozzle/vehicle sizing evaluations.

Utilization of the data base on the A/A vehicle concept is demonstrated for two of the tested nonaxisymmetric nozzle concepts and the P&WA axisymmetric baseline nozzle. The nonaxisymmetric concepts are a single expansion ramp nozzle, the GE aerodynamic load balanced exhaust nozzle (ALBEN), and a two-dimensional convergent-divergent nozzle, the P&WA 2-D C-D.

To illustrate basic differences in structural weights, vehicles were sized for the three different nozzle configurations with the same engine size (125 lb/s). This resulted in three vehicles which were identical in all particulars except nozzle installation and canard size, and which varied in TOGW from 25,873 lb for the axisymmetric nozzle, to 26,058 lb for the ALBEN and 26,143 lb for the 2-D C-D.

The vehicle structural weight for the three configurations differs only in type of nozzle installed and canard size. The GE ALBEN is 17 lb/nozzle heavier than the axisymmetric baseline, and the P&WA 2-D C-D is 59 lb/nozzle heavier when the engine is sized for 125 lb/s airflow. The larger canards, consistent with more unstable nonaxisymmetric vehicles, add an estimated 152 lb to the basic structural weight. The axisymmetric configuration incorporates a maximum unstable static margin of 10%, while the nonaxisymmetric vehicles are 15% unstable. None of the configurations were evaluated with the additional weight of a thrust reverser as there was no STOL requirement for the A/A vehicle.

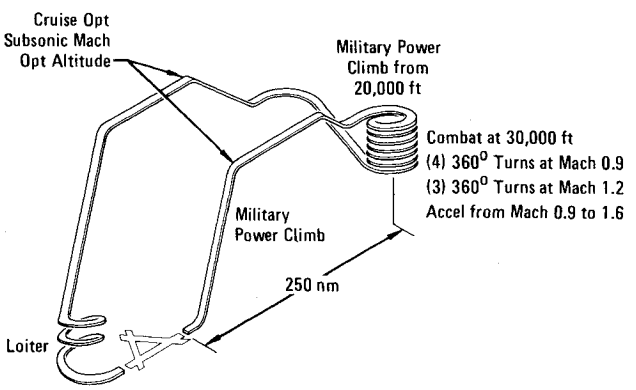

Fig. 2 Air-to-air mission and flight performance requirements.

Table 1 Important A/A mission segments

Segment	Mach/Altitude	Power setting
Transonic cruise	0.9/45 K ft	Reduced dry
Transonic combat	0.9/30 K ft	Maximum A/B
Supersonic combat	1.2/30 K ft	Maximum A/B

Aircraft Performance Prediction

Aircraft performance prediction for sizing evaluations usually involves separate buildup of the aerodynamic and propulsion characteristics. A schematic of the performance evaluation procedure recommended for use in conjunction with the test pod data base is illustrated in Fig. 4. The basic vehicle aerodynamics are evaluated for a "reference" configuration. The test pod data are used to assess nozzle internal performance as well as the "throttle-dependent" external force increments associated with engine operation at conditions different than the reference configuration. For the case of thrust vectoring, the test pod data are also used to assess thrust vector-induced effects on lift, drag, and trim characteristics.

Aerodynamic Performance

Prediction of the aerodynamic characteristics requires definition of a drag accounting system to adapt the test pod data to an arbitrary vehicle configuration. The reference geometry for the nozzle type under consideration has zero boattail projected area aft of the hinge point, and the nozzle operates at design nozzle pressure ratio (nozzle exit static pressure = freestream static pressure). Any nonnacelle structure in the nozzle vicinity is also included as part of the reference configuration, such as internozzle fairings or wing.

The vehicle reference drag is the sum of minimum profile drag ($C_{D_{MP}}$) and drag due to lift. The $C_{D_{MP}}$ estimate consists of friction and pressure (wave) drag for all configuration components. The estimated profile drag levels for the GE ALBEN, P&WA 2-D C-D, and axisymmetric nozzle/vehicle configurations are presented in Fig. 5. At subsonic speeds, the drag is highest for the 2-D C-D, reflecting the test pod empirical correction ($\Delta C_{D_{ref}}$) for the nozzle in the reference configuration. Supersonically, the $C_{D_{MP}}$ value primarily

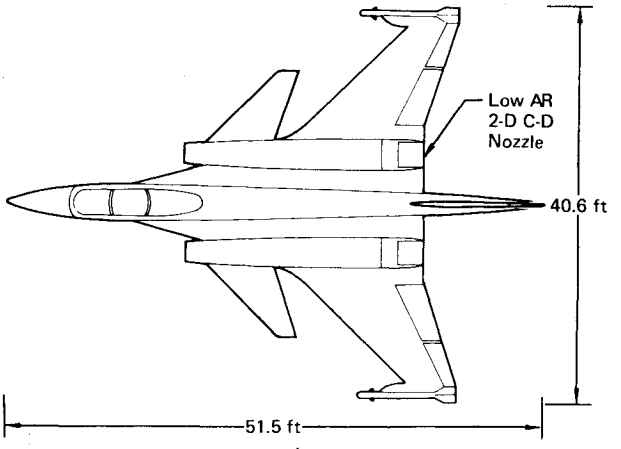

Payload . . . . . (2) Short Range Missiles, (2) Medium Range Missiles, and 20 mm Cannon
Inlets . . . . . Normal Shock
Engines . . . . . Mixed Flow Turbofans

Design Targets
- TOGW Class . . . . .30,000 lb
- $W/S_W]_{T/O}$ . . . . . 64 psf
- $T/W]_{T/O}$ 1.1
- Static Margin. . 15% Unstable

Fig. 3 Air-to-air vehicle concept.

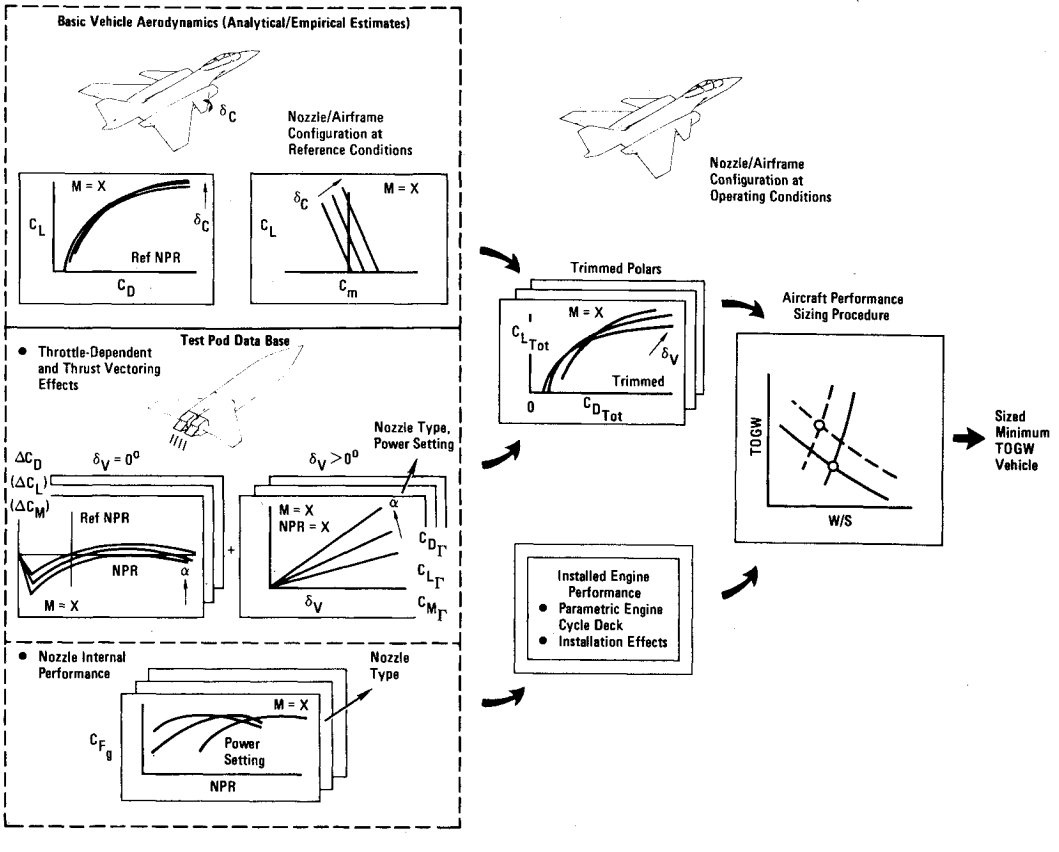

Fig. 4 Performance evaluation procedure

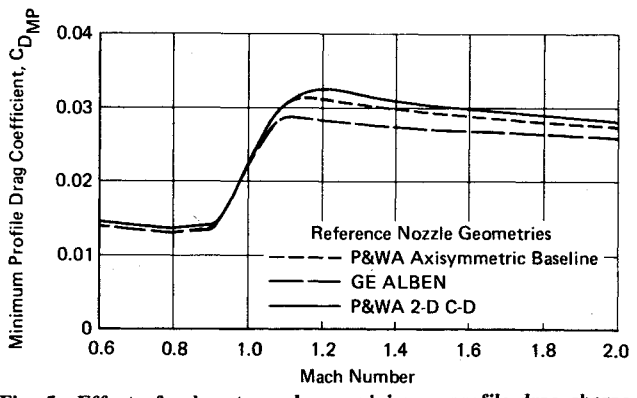

Fig. 5 Effect of exhaust nozzle on minimum profile drag characteristics; $S_w = 385$ ft^2, alt = 30,000 ft.

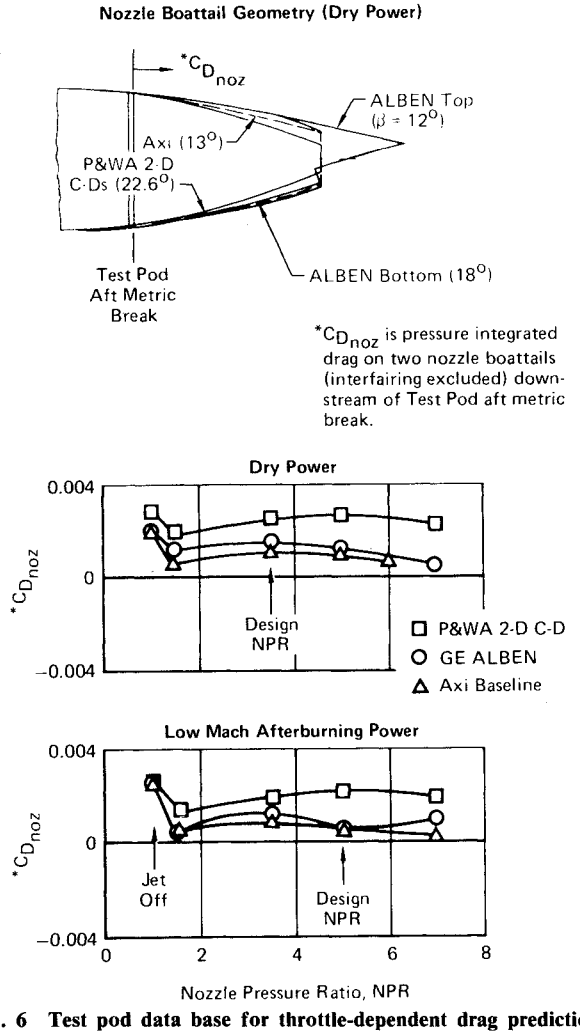

Fig. 6 Test pod data base for throttle-dependent drag prediction; Mach 0.9, $\alpha = 0$.

reflects differences in aftbody slope, with the nozzle with higher cross-sectional area at the nozzle hinge point having the lower slope and correspondingly lower wave drag.

The throttle-dependent effects are analyzed by considering the changes in the boattail pressure-integrated drags from the test pod nozzle installations. The test pod data base at $\alpha = 0$ deg for the two nonaxisymmetric nozzles and the axisymmetric baseline nozzle is shown in Fig. 6 at the dry and afterburning power settings corresponding to subsonic cruise and maneuver at Mach 0.9. The nozzle boattail drags ($C_{D_{noz}}$) of the axisymmetric and ALBEN nozzles are almost equal, while the drag of the 2-D C-D nozzle is higher due to higher boattail angles.

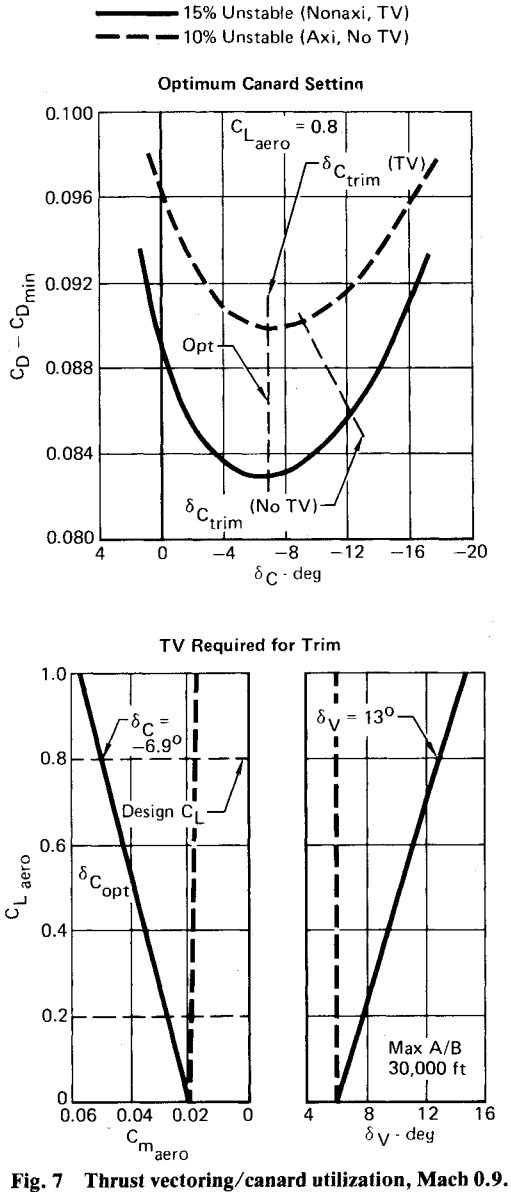

Fig. 7 Thrust vectoring/canard utilization, Mach 0.9.

The throttle-dependent effects can also be dependent on angle of attack. The test pod data revealed that the drag of the axisymmetric nozzle increased more rapidly with angle of attack than that of the nonaxisymmetric nozzles, particularly at dry power. For example, $C_{D_{noz}}$ for the dry power axisymmetric nozzle increased 34 counts ($\Delta C_{D_{noz}} = 0.0034$) at Mach 0.9 between $\alpha = 0$ and 6.4 deg, which is the subsonic cruise angle of attack for the A/A vehicle. The boattail drag of the P&WA 2-D C-D increased about one-half this amount. In addition, there is a beneficial increment in lift on the boattail of the GE ALBEN, which cannot be ignored in sizing evaluations when compared to the lift on the axisymmetric nozzle boattail.

Thrust vectoring can provide a beneficial lift/drag effect at subsonic maneuver conditions when used synergistically with the horizontal canard. A design objective for the A/A vehicle was to tailor the vehicle pitching moment characteristics at the Mach 0.9 sustained turn condition (6 g at 30,000 ft) to achieve an untrimmed, nose-up moment at the canard deflection for minimum drag. Positive thrust vectoring is then used for trim, producing a beneficial lift/drag ratio increment from supercirculation.

Utilization of thrust vectoring for trim at the optimum canard setting is illustrated in Fig. 7 for two different static margin levels. The static margin difference was accomplished

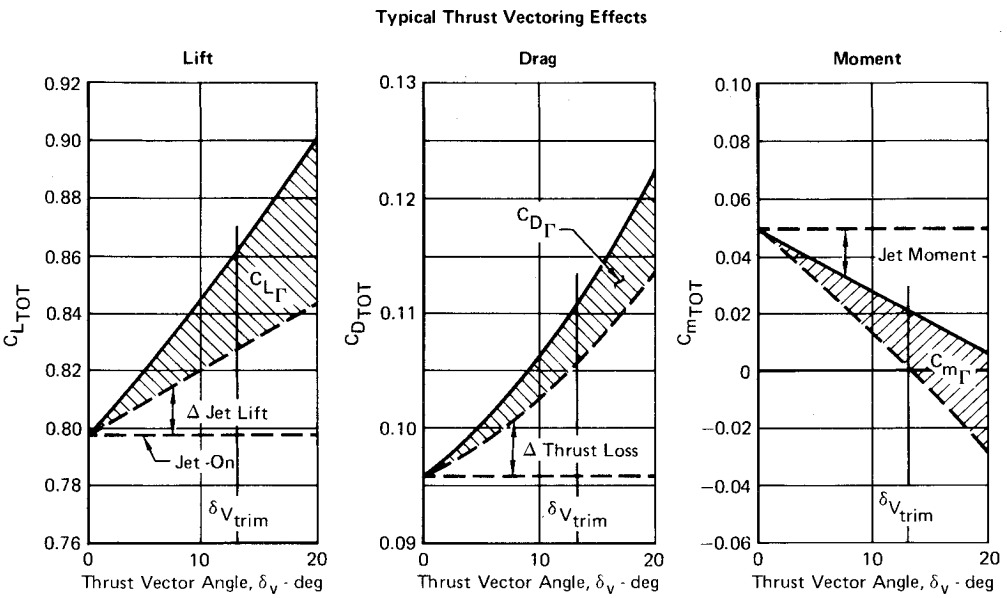

Fig. 8 Prediction of thrust vectoring effects on longitudinal aerodynamics; 15% unstable, max A/B, Mach 0.9, $\alpha = 11$ deg.

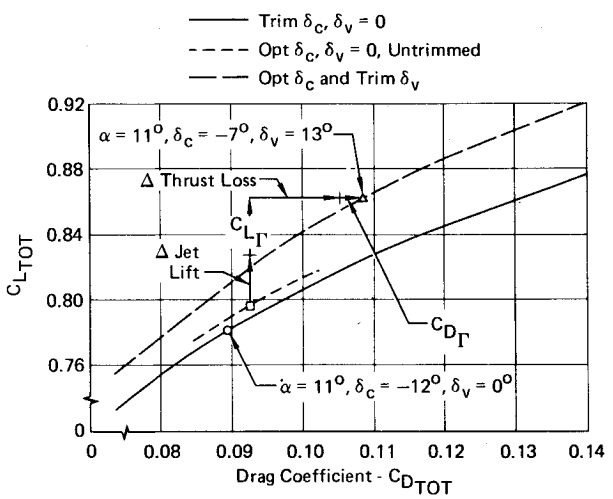

Fig. 9 Effect of thrust vectoring on trimmed polar; air-to-air, 15% unstable, Mach 0.9 at 30,000 ft, max A/B.

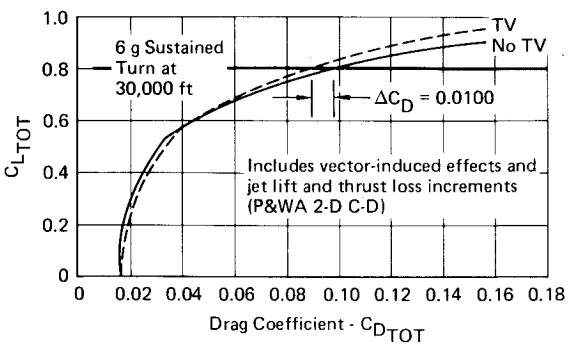

Fig. 10 Thrust vectoring improves trimmed polar above "drag break"; Mach 0.9, max A/B, 15% unstable.

by increasing the canard size about 50%, while maintaining constant wing area and location. The 15% $\bar{c}$ unstable case yields lower drag due to lift because the larger canard contributes a greater portion of the total lift, thereby decreasing the induced drag of the wing/canard combination. However, a residual nose-up pitching moment is produced at the optimum (minimum drag) canard setting, as also shown in Fig. 7. This nose-up moment is larger at the more relaxed static margin level, thus requiring more nozzle deflection to trim for the 15% $\bar{c}$ unstable case. (Trim nozzle deflection increases from 6 to 13 deg.) The advantage of trimmed drag due to lift for the more unstable configuration when used with thrust vectoring is offset somewhat by increased weight and higher profile drag of the larger canard. These effects are accounted for in the sizing analysis.

The thrust vectoring payoff at 15% $\bar{c}$ unstable can be demonstrated by comparing trimmed drag polars, with and without vectoring, at the Mach 0.9 sustained turn condition. To establish the trimmed polars, the vector-induced lift, drag, and pitching moment effects are first determined and then applied to the estimated A/A vehicle untrimmed polar for the optimum canard setting case. The vector-induced effects are predicted from correlations of the test pod data.[1] The predicted induced effects on the longitudinal aerodynamics of the A/A vehicle are shown in Fig. 8 as well as the direct jet lift, thrust loss, and jet moment increments.

Application of the vectoring increments to the untrimmed polar is illustrated in Fig. 9 for the region of the polar near the sustained turn lift coefficient. The vector-induced lift and drag increments and the jet lift and thrust loss increments corresponding to the nozzle deflection required for trim (13 deg) are added to produce the trimmed drag polar with thrust vectoring. The trimmed drag polars, with and without thrust vectoring, for the complete C_L range at Mach 0.9 are shown in Fig. 10. Note that thrust vectoring improves the trimmed drag polar above "drag break," which is the point at which wing flow separation begins. Thrust vectoring provides a substantial drag advantage ($\Delta C_D = 0.0100$) for a sustained turn at 30,000 ft.

Figures 8-10 illustrate the beneficial results if a vectorable nonaxisymmetric nozzle is properly integrated into the trailing edge of a wing. The flow exhausting from the nozzle favorably influences the flow around the wing which results in improved lift and drag characteristics. Both vectored and thrust-induced lift contribute to this improvement. A vectorable axisymmetric nozzle would not integrate into the wing trailing edge as well and would contribute very little thrust-induced lift or supercirculation.

Gross Thrust Performance

The nozzle related effects on gross thrust are analyzed by considering the installed gross thrust coefficient ($C_{F_{gins}}$) plus any nozzle cooling effects which act to change the gross thrust available at maximum afterburning power ($\Delta F_{g_{max}}$). The installed gross thrust coefficient is obtained by modifying the model (test pod) C_{F_g} values for the effects of leakage and

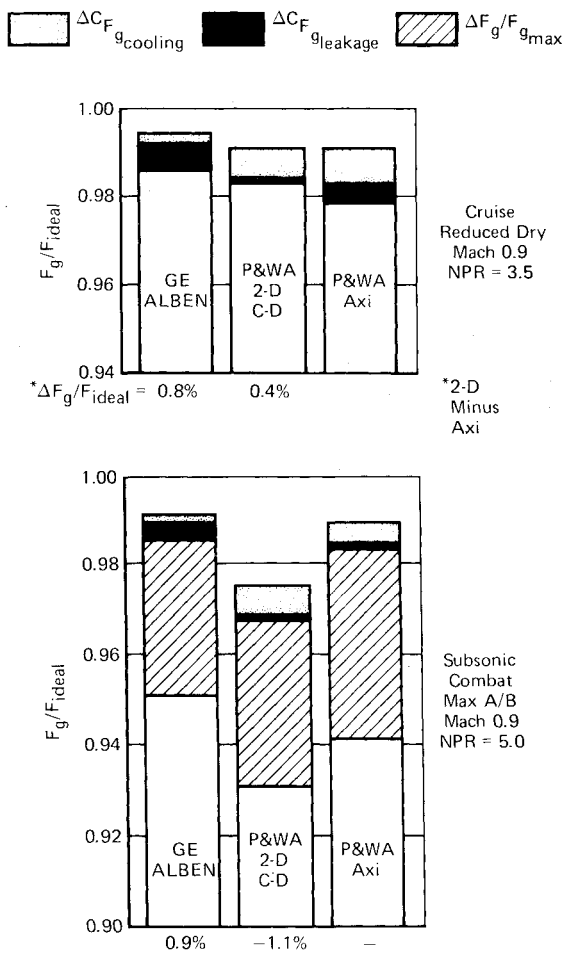

Fig. 11 Gross thrust predictions, $\delta_N = 0$ deg.

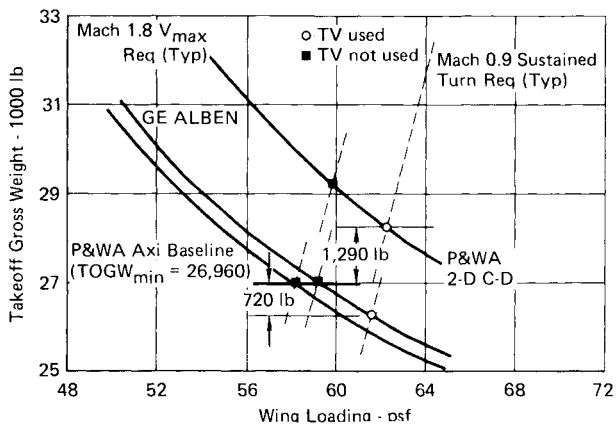

Fig. 12 Final sizing results.

cooling, i.e.,

$$C_{F_{g_{ins}}} = C_{F_{g_{model}}} + \Delta C_{g\ leakage} + \Delta C_{F_{g_{cooling}}}$$

The model C_{F_g} values for sizing analysis are obtained by modifying the absolute static C_{F_g} levels for the incremental effects of external flow and/or vectoring. Considering the two nonaxisymmetric and axisymmetric nozzles, incremental external flow effects on $C_{F_{g_{model}}}$ were observed only for the ALBEN, which incorporates the single external expansion ramp. This is due to a favorable recompression effect of the external flow on the partially subsonic flow over the exposed expansion surfaces.

The nozzle cooling and leakage effects on $C_{F_{g_{ins}}}$ are provided from engine company estimates on the full-scale designs. There is a cooling penalty on the thrust coefficient due to pressure losses and/or nozzle exit momentum losses related to the coolant flowrate and cooling techniques employed in the full-scale designs. The nonaxisymmetric nozzle cooling penalties are generally equal to or less than those of the axisymmetric nozzles. This is an indication of efficient cooling designs for the nonaxisymmetric nozzles since the surface areas which must be cooled are typically greater. The leakage penalties for the nonaxisymmetric nozzles are also generally equal to or less than those of the axisymmetric case. This is the result of greater seal length requirements for the multiple flap axisymmetric nozzle.

A summary of all nozzle reflected effects on gross thrust for two important operating points of the A/A vehicle is shown in Fig. 11. In general, the performance of the GE ALBEN is competitive with the axisymmetric baseline nozzle, with the largest difference being 0.9% in favor of the ALBEN. However, at supersonic conditions, the gross thrust of the P&WA 2-D C-D nozzle is up to 2.3% lower than the baseline. This is due to the short divergent flap length of the 2-D C-D, which results in a lightweight design but at the expense of maximum internal area ratio.

Vehicle Sizing Results

The nozzle related weight, drag, and gross thrust estimates were combined with the overall vehicle characteristics in a computerized engine/airframe sizing procedure to determine the aircraft TOGW required to meet the A/A mission and flight performance requirements. Each configuration was evaluated at two levels of maximum unstable static margin, 10 and 15% $\bar{c}$. The minimum TOGW for the two nonaxisymmetric nozzle/vehicle installations, utilizing thrust vectoring for trimming at high lift coefficients, was obtained for the 15% unstable case. The TOGW of the baseline axisymmetric nozzle/vehicle configuration without thrust vectoring was a minimum at 10% unstable static margin. These results were not unexpected since favorable thrust vectoring effects act to offset the canard size penalties associated with the more unstable configuration.

The sizing results are presented in Fig. 12 as a function of wing loading for the static margin, resulting in the minimum TOGW for each configuration. These results show that the GE ALBEN installation with thrust vectoring is about 2.6% (720 lb) lighter than the axisymmetric baseline configuration; the P&WA 2-D C-D installation is about 4.8% (1290 lb) heavier than the baseline.

The lower TOGW of the ALBEN configuration is primarily due to significantly lower drag at the subsonic combat flight condition. This results from a combination of thrust vectoring for supercirculation and optimum canard trim, plus favorable nozzle lift/drag characteristics at unvectored conditions. These effects occur at moderate to high angles of attack (6-12 deg). The nozzle gross thrust and weight differences between the ALBEN and the P&WA baseline axisymmetric nozzle contribute relatively little to the TOGW difference. The P&WA 2-D C-D nozzle, however, shows a significant drag advantage compared to the baseline only at the subsonic combat point. This advantage is more than offset by the gross thrust and drag penalties incurred supersonically and the nozzle weight penalty.

Conclusions

A substantial data base has been provided to quantify the design and aerodynamic performance characteristics of low aspect ratio, nonaxisymmetric nozzles, and the vehicle performance of an advanced fighter has been evaluated utilizing this data base.

For the A/A mission, a higher TOGW of about 4.8% was estimated for the P&WA 2-D C-D nozzle/vehicle with thrust vectoring, compared to the baseline axisymmetric configuration without thrust vectoring. The higher TOGW was primarily due to the lower supersonic internal performance associated with reduced area ratio capability. Considering the ALBEN nozzle/vehicle vs the axisymmetric nozzle/vehicle, the nonaxisymmetric configuration was lighter by 2.6%. This was due to the lightweight nozzle design and lower installation drag plus the use of 13 deg of thrust vectoring at maneuver conditions. Effective utilization of thrust vectoring required relaxation of the static margin to 15% $\bar{c}$ unstable, compared to 10% $\bar{c}$ unstable for the axisymmetric configuration without thrust vectoring.

References

[1] Hiley, P.E., et al., "Experimental Evaluation of Non-Axisymmetric Exhaust Nozzles," Vols. I & II, McDonnell Aircraft Co., St. Louis, Mo., Final Report AFFDL-TR-78-185, Dec. 1978.

[2] Willard, C.M., et al., "Static Performance of Vectoring/Reversing Non-Axisymmetric Nozzles," AIAA Paper 77-840, AIAA/SAE 13th Joint Propulsion Conference, Orlando, Fla., July 1977.

[3] Capone, F.J., "Static Performance of Five Twin Engine Non-Axisymmetric Nozzles with Vectoring and Reversing Capability," NASA TP 1224, July 1978.

[4] Hiley, P.E., Kitzmiller, D.E., and Willard, C.M., "Installed Performance of Vectoring/Reversing Non-Axisymmetric Nozzles," AIAA Paper 78-1022, AIAA/SAE 14th Joint Propulsion Conference, Las Vegas, Nev., July 1978.